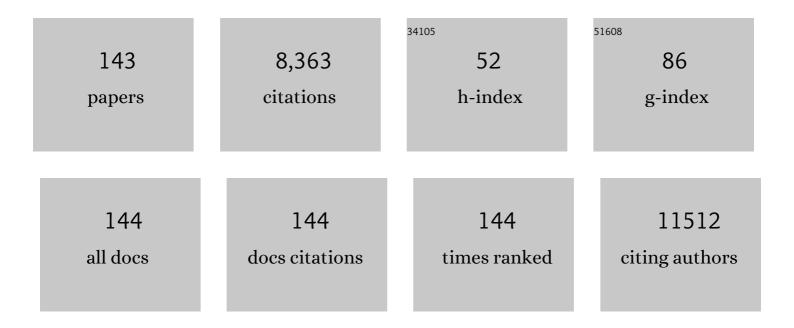
Zhihui Dai

List of Publications by Year in descending order

Source: https://exaly.com/author-pdf/980887/publications.pdf Version: 2024-02-01



ΖΗΙΗΠΙ ΠΛΙ

#	Article	IF	CITATIONS
1	Pomegranate-like N,P-Doped Mo ₂ C@C Nanospheres as Highly Active Electrocatalysts for Alkaline Hydrogen Evolution. ACS Nano, 2016, 10, 8851-8860.	14.6	575
2	Ru Modulation Effects in the Synthesis of Unique Rod-like Ni@Ni ₂ P–Ru Heterostructures and Their Remarkable Electrocatalytic Hydrogen Evolution Performance. Journal of the American Chemical Society, 2018, 140, 2731-2734.	13.7	326
3	Two-Dimensional Tin Selenide Nanostructures for Flexible All-Solid-State Supercapacitors. ACS Nano, 2014, 8, 3761-3770.	14.6	322
4	Nanostructured FeS as a Mimic Peroxidase for Biocatalysis and Biosensing. Chemistry - A European Journal, 2009, 15, 4321-4326.	3.3	291
5	Co ₃ S ₄ porous nanosheets embedded in graphene sheets as high-performance anode materials for lithium and sodium storage. Journal of Materials Chemistry A, 2015, 3, 6787-6791.	10.3	247
6	2D Electron Gas and Oxygen Vacancy Induced High Oxygen Evolution Performances for Advanced Co ₃ O ₄ /CeO ₂ Nanohybrids. Advanced Materials, 2019, 31, e1900062.	21.0	242
7	Wet milled synthesis of an Sb/MWCNT nanocomposite for improved sodium storage. Journal of Materials Chemistry A, 2013, 1, 13727.	10.3	188
8	Electrochemiluminescence for Electric-Driven Antibacterial Therapeutics. Journal of the American Chemical Society, 2018, 140, 2284-2291.	13.7	180
9	Metal–organic framework templated nitrogen and sulfur co-doped porous carbons as highly efficient metal-free electrocatalysts for oxygen reduction reactions. Journal of Materials Chemistry A, 2014, 2, 6316-6319.	10.3	179
10	Defectâ€Rich Ni ₃ FeN Nanocrystals Anchored on Nâ€Đoped Graphene for Enhanced Electrocatalytic Oxygen Evolution. Advanced Functional Materials, 2018, 28, 1706018.	14.9	169
11	Fluorine-Doped Carbon Particles Derived from Lotus Petioles as High-Performance Anode Materials for Sodium-Ion Batteries. Journal of Physical Chemistry C, 2015, 119, 21336-21344.	3.1	158
12	Immobilization and direct electrochemistry of glucose oxidase on a tetragonal pyramid-shaped porous ZnO nanostructure for a glucose biosensor. Biosensors and Bioelectronics, 2009, 24, 1286-1291.	10.1	139
13	A selenium-confined microporous carbon cathode for ultrastable lithium–selenium batteries. Journal of Materials Chemistry A, 2014, 2, 17735-17739.	10.3	117
14	Cesium Lead Halide Perovskite Quantum Dots as a Photoluminescence Probe for Metal Ions. Advanced Materials, 2017, 29, 1700150.	21.0	112
15	Using Graphene-Based Plasmonic Nanocomposites to Quench Energy from Quantum Dots for Signal-On Photoelectrochemical Aptasensing. Analytical Chemistry, 2013, 85, 11720-11724.	6.5	108
16	An Improved Ultrasensitive Enzyme-Linked Immunosorbent Assay Using Hydrangea-Like Antibody–Enzyme–Inorganic Three-in-One Nanocomposites. ACS Applied Materials & Interfaces, 2016, 8, 6329-6335.	8.0	104
17	A bienzyme channeling glucose sensor with a wide concentration range based on co-entrapment of enzymes in SBA-15 mesopores. Biosensors and Bioelectronics, 2008, 23, 1070-1076.	10.1	100
18	Five-Fold Twinned Pd ₂ NiAg Nanocrystals with Increased Surface Ni Site Availability to Improve Oxygen Reduction Activity. Journal of the American Chemical Society, 2015, 137, 2820-2823.	13.7	100

#	Article	IF	CITATIONS
19	Selective photoelectrochemical architectures for biosensing: Design, mechanism and responsibility. TrAC - Trends in Analytical Chemistry, 2018, 105, 470-483.	11.4	97
20	Photoelectrochemical Biosensor Using Enzyme-Catalyzed in Situ Propagation of CdS Quantum Dots on Graphene Oxide. ACS Applied Materials & Interfaces, 2014, 6, 16197-16203.	8.0	96
21	Electrochemiluminescence Tuned by Electron–Hole Recombination from Symmetry-Breaking in Wurtzite ZnSe. Journal of the American Chemical Society, 2016, 138, 1154-1157.	13.7	96
22	Integrating ultrathin and modified NiCoAl-layered double-hydroxide nanosheets with N-doped reduced graphene oxide for high-performance all-solid-state supercapacitors. Nanoscale, 2019, 11, 9896-9905.	5.6	95
23	In Situ-Generated Nano-Gold Plasmon-Enhanced Photoelectrochemical Aptasensing Based on Carboxylated Perylene-Functionalized Graphene. Analytical Chemistry, 2014, 86, 1306-1312.	6.5	93
24	Fluorescence Regulation of Poly(thymine)-Templated Copper Nanoparticles via an Enzyme-Triggered Reaction toward Sensitive and Selective Detection of Alkaline Phosphatase. Analytical Chemistry, 2017, 89, 3681-3686.	6.5	93
25	Ge Nanoparticles Encapsulated in Nitrogen-Doped Reduced Graphene Oxide as an Advanced Anode Material for Lithium-Ion Batteries. Journal of Physical Chemistry C, 2014, 118, 28502-28508.	3.1	92
26	Aggregation of Individual Sensing Units for Signal Accumulation: Conversion of Liquid-Phase Colorimetric Assay into Enhanced Surface-Tethered Electrochemical Analysis. Journal of the American Chemical Society, 2015, 137, 8880-8883.	13.7	92
27	Coralloid Co ₂ P ₂ O ₇ Nanocrystals Encapsulated by Thin Carbon Shells for Enhanced Electrochemical Water Oxidation. ACS Applied Materials & Interfaces, 2016, 8, 22534-22544.	8.0	91
28	Preparation of Silicon–Carbon-Based Dots@Dopamine and Its Application in Intracellular Ag ⁺ Detection and Cell Imaging. ACS Applied Materials & Interfaces, 2016, 8, 3644-3650.	8.0	91
29	Construction of Molecular Sensing and Logic Systems Based on Site-Occupying Effect-Modulated MOF–DNA Interaction. Journal of the American Chemical Society, 2020, 142, 21267-21271.	13.7	87
30	Dual Signal Amplification Using Gold Nanoparticles-Enhanced Zinc Selenide Nanoflakes and P19 Protein for Ultrasensitive Photoelectrochemical Biosensing of MicroRNA in Cell. Analytical Chemistry, 2016, 88, 10459-10465.	6.5	85
31	An Electrochemical Biosensor with Dual Signal Outputs: Toward Simultaneous Quantification of pH and O ₂ in the Brain upon Ischemia and in a Tumor during Cancer Starvation Therapy. Angewandte Chemie - International Edition, 2017, 56, 10471-10475.	13.8	84
32	Facile synthesis of high-quality nano-sized CdS hollow spheres and their application in electrogenerated chemiluminescence sensing. Journal of Materials Chemistry, 2007, 17, 1087-1093.	6.7	83
33	Mild Hyperthermia-Enhanced Enzyme-Mediated Tumor Cell Chemodynamic Therapy. ACS Applied Materials & Interfaces, 2019, 11, 23065-23071.	8.0	77
34	Near-Infrared Light Excited and Localized Surface Plasmon Resonance-Enhanced Photoelectrochemical Biosensing Platform for Cell Analysis. Analytical Chemistry, 2018, 90, 9403-9409.	6.5	74
35	Synergistically enhanced oxygen reduction electrocatalysis by atomically dispersed and nanoscaled Co species in three-dimensional mesoporous Co, N-codoped carbon nanosheets network. Applied Catalysis B: Environmental, 2020, 260, 118207.	20.2	74
36	A novel nitrite biosensor based on the direct electron transfer of hemoglobin immobilized on CdS hollow nanospheres. Biosensors and Bioelectronics, 2008, 23, 1869-1873.	10.1	73

#	Article	IF	CITATIONS
37	Fe-Porphyrin-Based Covalent Organic Framework As a Novel Peroxidase Mimic for a One-Pot Glucose Colorimetric Assay. ACS Applied Bio Materials, 2018, 1, 382-388.	4.6	72
38	A facile synthesis of PdCo bimetallic hollow nanospheres and their application to Sonogashira reaction in aqueous media. New Journal of Chemistry, 2006, 30, 832.	2.8	71
39	Two-dimensional nanostructures of non-layered ternary thiospinels and their bifunctional electrocatalytic properties for oxygen reduction and evolution: the case of CuCo ₂ S ₄ nanosheets. Inorganic Chemistry Frontiers, 2016, 3, 1501-1509.	6.0	69
40	Photo-tearable tape close-wrapped upconversion nanocapsules for near-infrared modulated efficient siRNA delivery and therapy. Biomaterials, 2018, 163, 55-66.	11.4	69
41	Well-Coupled Graphene and Pd-Based Bimetallic Nanocrystals Nanocomposites for Electrocatalytic Oxygen Reduction Reaction. ACS Applied Materials & Interfaces, 2014, 6, 2086-2094.	8.0	67
42	Ratiometric Fluorescent Quantum Dot-Based Biosensor for Chlorothalonil Detection via an Inner-Filter Effect. Analytical Chemistry, 2020, 92, 4364-4370.	6.5	67
43	Simultaneous and ultrasensitive detection of three pesticides using a surface-enhanced Raman scattering-based lateral flow assay test strip. Biosensors and Bioelectronics, 2021, 181, 113149.	10.1	67
44	Ultralong Cycle Life Sodium-Ion Battery Anodes Using a Graphene-Templated Carbon Hybrid. Journal of Physical Chemistry C, 2014, 118, 22426-22431.	3.1	66
45	Polarized Optoelectronics of CsPbX ₃ (X = Cl, Br, I) Perovskite Nanoplates with Tunable Size and Thickness. Advanced Functional Materials, 2018, 28, 1800283.	14.9	63
46	Photoelectrochemical Bioanalysis Platform for Cells Monitoring Based on Dual Signal Amplification Using in Situ Generation of Electron Acceptor Coupled with Heterojunction. ACS Applied Materials & Interfaces, 2017, 9, 22289-22297.	8.0	62
47	Enhancing the Anode Performance of Antimony through Nitrogen-Doped Carbon and Carbon Nanotubes. Journal of Physical Chemistry C, 2016, 120, 3214-3220.	3.1	61
48	Component-Controlled Synthesis and Assembly of Cu–Pd Nanocrystals on Graphene for Oxygen Reduction Reaction. ACS Applied Materials & Interfaces, 2015, 7, 5347-5357.	8.0	60
49	Component-Controlled Synthesis of Necklace-Like Hollow Ni _{<i>X</i>} Ru _{<i>y</i>} Nanoalloys as Electrocatalysts for Hydrogen Evolution Reaction. ACS Applied Materials & Interfaces, 2017, 9, 17326-17336.	8.0	60
50	Construction of Metal-Ion-Free G-quadruplex-Hemin DNAzyme and Its Application in S1 Nuclease Detection. ACS Applied Materials & amp; Interfaces, 2016, 8, 827-833.	8.0	56
51	Mesoporous Materials Promoting Direct Electrochemistry and Electrocatalysis of Horseradish Peroxidase. Electroanalysis, 2005, 17, 862-868.	2.9	55
52	A carbon nanotube/quantum dot based photoelectrochemical biosensing platform for the direct detection of microRNAs. Chemical Communications, 2014, 50, 13315-13318.	4.1	55
53	3D Porous Nanoarchitectures Derived from SnS/Sâ€Doped Graphene Hybrid Nanosheets for Flexible Allâ€Solidâ€State Supercapacitors. Small, 2017, 13, 1603494.	10.0	55
54	Engineering Mo/Mo ₂ C/MoC hetero-interfaces for enhanced electrocatalytic nitrogen reduction. Journal of Materials Chemistry A, 2020, 8, 8920-8926.	10.3	54

#	Article	IF	CITATIONS
55	Fabrication of Hierarchical Nanostructure of Silver via a Surfactant-Free Mixed Solvents Route. Crystal Growth and Design, 2009, 9, 3941-3947.	3.0	52
56	Conjugated Polymer-Based Photoelectrochemical Cytosensor with Turn-On Enable Signal for Sensitive Cell Detection. ACS Applied Materials & amp; Interfaces, 2018, 10, 6618-6623.	8.0	52
57	A novel tetragonal pyramid-shaped porous ZnO nanostructure and its application in the biosensing of horseradish peroxidase. Journal of Materials Chemistry, 2008, 18, 1919.	6.7	51
58	In situ generated AgBr-enhanced ZnO nanorod-based photoelectrochemical aptasensing via layer-by-layer assembly. Chemical Communications, 2014, 50, 2108.	4.1	51
59	Quantum dots sensitized titanium dioxide decorated reduced graphene oxide for visible light excited photoelectrochemical biosensing at a low potential. Biosensors and Bioelectronics, 2014, 54, 331-338.	10.1	49
60	Label-free photoelectrochemical cytosensing via resonance energy transfer using gold nanoparticle-enhanced carbon dots. Chemical Communications, 2015, 51, 14259-14262.	4.1	49
61	Fluorescence Regulation of Copper Nanoclusters via DNA Template Manipulation toward Design of a High Signal-to-Noise Ratio Biosensor. ACS Applied Materials & Interfaces, 2018, 10, 6965-6971.	8.0	47
62	Detection of Trace Phenol Based on Mesoporous Silica Derived Tyrosinase-Peroxidase Biosensor. Electroanalysis, 2005, 17, 1571-1577.	2.9	46
63	A localized surface plasmon resonance-enhanced photoelectrochemical biosensing strategy for highly sensitive and scatheless cell assay under red light excitation. Chemical Communications, 2016, 52, 11799-11802.	4.1	45
64	Red light-driven photoelectrochemical biosensing for ultrasensitive and scatheless assay of tumor cells based on hypotoxic AgInS2 nanoparticles. Biosensors and Bioelectronics, 2019, 126, 332-338.	10.1	44
65	Bimetallic metal–organic framework for enzyme immobilization by biomimetic mineralization: Constructing a mimic enzyme and simultaneously immobilizing natural enzymes. Analytica Chimica Acta, 2020, 1098, 148-154.	5.4	42
66	Rapid and sensitive detection of microRNA via the capture of fluorescent dyes-loaded albumin nanoparticles around functionalized magnetic beads. Biosensors and Bioelectronics, 2017, 94, 56-62.	10.1	41
67	Two-dimensional porous γ-AlOOH and γ-Al ₂ O ₃ nanosheets: hydrothermal synthesis, formation mechanism and catalytic performance. RSC Advances, 2015, 5, 71728-71734.	3.6	40
68	A silver@gold nanoparticle tetrahedron biosensor for multiple pesticides detection based on surface-enhanced Raman scattering. Talanta, 2021, 234, 122585.	5.5	38
69	Enhancing Photoelectric Response of an Au@Ag/AgI Schottky Contact through Regulation of Localized Surface Plasmon Resonance. Journal of the American Chemical Society, 2021, 143, 13478-13482.	13.7	37
70	A "Signal On―Photoelectrochemical Biosensor Based on Bismuth@N,O odoped arbon Coreâ€6hell Nanohybrids for Ultrasensitive Detection of Telomerase in HeLa Cells. Chemistry - A European Journal, 2018, 24, 3677-3682.	3.3	35
71	Alternate Integration of Vertically Oriented CuSe@FeOOH and CuSe@MnOOH Hybrid Nanosheets Frameworks for Flexible In-Plane Asymmetric Micro-supercapacitors. ACS Applied Energy Materials, 2020, 3, 3692-3703.	5.1	35
72	Electrochemical Immunoassays Based on Graphene: A Review. Electroanalysis, 2016, 28, 4-12.	2.9	34

#	Article	IF	CITATIONS
73	Triple-Helix Molecular Switch Electrochemiluminescence Nanoamplifier Based on a S-Doped Lu ₂ O ₃ /Ag ₂ S Pair for Sensitive MicroRNA Detection. Analytical Chemistry, 2019, 91, 12038-12045.	6.5	33
74	Constructing Heterostructured Bimetallic Selenides on an N-Doped Carbon Nanoframework as Anodes for Ultrastable Na-Ion Batteries. ACS Applied Materials & Interfaces, 2022, 14, 1222-1232.	8.0	33
75	Modulating Polarization of Perovskite-Based Heterostructures via In Situ Semiconductor Generation and Enzyme Catalysis for Signal-Switchable Photoelectrochemical Biosensing. Analytical Chemistry, 2021, 93, 8370-8378.	6.5	32
76	Formation of a Photoelectrochemical <i>Z</i> -Scheme Structure with Inorganic/Organic Hybrid Materials for Evaluation of Receptor Protein Expression on the Membrane of Cancer Cells. ACS Applied Materials & Interfaces, 2020, 12, 26905-26913.	8.0	31
77	Ultrasensitive electrochemical biosensing for DNA using quantum dots combined with restriction endonuclease. Analyst, The, 2015, 140, 506-511.	3.5	29
78	Stable and Reusable Electrochemical Biosensor for Poly(ADP-ribose) Polymerase and Its Inhibitor Based on Enzyme-Initiated Auto-PARylation. ACS Applied Materials & Interfaces, 2016, 8, 18669-18674.	8.0	29
79	Cucurbituril and Azide Cofunctionalized Graphene Oxide for Ultrasensitive Electro-Click Biosensing. Analytical Chemistry, 2017, 89, 12237-12243.	6.5	29
80	Electrochemical Assay of the Alpha Fetoprotein-L3 Isoform Ratio To Improve the Diagnostic Accuracy of Hepatocellular Carcinoma. Analytical Chemistry, 2018, 90, 13051-13058.	6.5	29
81	CdSe quantum dots as labels for sensitive immunoassay of cancer biomarker proteins by electrogenerated chemiluminescence. Analyst, The, 2011, 136, 5197.	3.5	28
82	Electrochemical monitoring of an important biomarker and target protein: VEGFR2 in cell lysates. Scientific Reports, 2014, 4, 3982.	3.3	28
83	Low Potential Detection of NADH at Titanium-Containing MCM-41â€Modified Glassy Carbon Electrode. Electroanalysis, 2007, 19, 604-607.	2.9	27
84	Componentâ€Controlled Synthesis of Smallâ€Sized Pdâ€Ag Bimetallic Alloy Nanocrystals and Their Application in a Nonâ€Enzymatic Glucose Biosensor. Particle and Particle Systems Characterization, 2013, 30, 549-556.	2.3	27
85	SbSI Nanocrystals: An Excellent Visible Light Photocatalyst with Efficient Generation of Singlet Oxygen. ACS Sustainable Chemistry and Engineering, 2018, 6, 12166-12175.	6.7	27
86	Component reconstitution-driven photoelectrochemical sensor for sensitive detection of Cu2+ based on advanced CuS/CdS p-n junction. Science China Chemistry, 2019, 62, 1725-1731.	8.2	26
87	Oxidase-mimicking activity of ultrathin MnO2 nanosheets in a colorimetric assay of chlorothalonil in food samples. Food Chemistry, 2020, 331, 127090.	8.2	26
88	Aggregation-induced fluorescence probe for hypochlorite imaging in mitochondria of living cells and zebrafish. Journal of Materials Chemistry B, 2020, 8, 7375-7381.	5.8	26
89	Near-infrared MnCuInS/ZnS@BSA and urchin-like Au nanoparticle as a novel donor-acceptor pair for enhanced FRET biosensing. Analytica Chimica Acta, 2018, 1042, 71-78.	5.4	25
90	Photoelectrochemical Approach to Apoptosis Evaluation via Multi-Functional Peptide- and Electrostatic Attraction-Guided Excitonic Response. Analytical Chemistry, 2019, 91, 830-835.	6.5	25

#	Article	IF	CITATIONS
91	Engineering bimetal Cu, Co sites on 3D N-doped porous carbon nanosheets for enhanced oxygen reduction electrocatalysis. Chemical Communications, 2020, 56, 10010-10013.	4.1	25
92	Quantification of cyclic DNA polymerization with lanthanide coordination nanomaterials for liquid biopsy. Chemical Science, 2020, 11, 3745-3751.	7.4	25
93	Highly sensitive "signal-on―electrochemiluminescent biosensor for the detection of DNA based on dual quenching and strand displacement reaction. Chemical Communications, 2015, 51, 14578-14581.	4.1	24
94	Significantly Enhanced Hydrogen Evolution Activity of Freestanding Pdâ€Ru Distorted Icosahedral Clusters with less than 600 Atoms. Chemistry - A European Journal, 2017, 23, 18203-18207.	3.3	24
95	Applications of DNA-nanozyme-based sensors. Analyst, The, 2021, 146, 1127-1141.	3.5	24
96	An amperometric glucose biosensor constructed by immobilizing glucose oxidase on titanium-containing mesoporous composite material of no. 41 modified screen-printed electrodes. Analytica Chimica Acta, 2007, 591, 195-199.	5.4	23
97	Electrochemiluminescence of CdSe quantum dots for highly sensitive competitive immunosensing. Sensors and Actuators B: Chemical, 2012, 168, 271-276.	7.8	23
98	Sequence and Structure Dual-Dependent Interaction between Small Molecules and DNA for the Detection of Residual Silver Ions in As-Prepared Silver Nanomaterials. Analytical Chemistry, 2017, 89, 6815-6820.	6.5	23
99	Graphene Oxideâ€Assisted and DNAâ€Modulated SERS of AuCu Alloy for the Fabrication of Apurinic/Apyrimidinic Endonuclease 1 Biosensor. Small, 2019, 15, e1901506.	10.0	23
100	Dual-path modulation of hydrogen peroxide to ameliorate hypoxia for enhancing photodynamic/starvation synergistic therapy. Journal of Materials Chemistry B, 2020, 8, 9933-9942.	5.8	22
101	Green light excited ultrasensitive photoelectrochemical biosensing for microRNA at a low applied potential based on the dual role of Au NPs in TiO ₂ nanorods/Au NPs composites. Nanoscale, 2018, 10, 16474-16478.	5.6	21
102	Amino Acid-Capped Water-Soluble Near-Infrared Region CuInS2/ZnS Quantum Dots for Selective Cadmium Ion Determination and Multicolor Cell Imaging. Analytical Chemistry, 2019, 91, 8987-8993.	6.5	21
103	Well-Coupled Nanohybrids Obtained by Component-Controlled Synthesis and in Situ Integration of Mn _{<i>x</i>} Pd _{<i>y</i>} Nanocrystals on Vulcan Carbon for Electrocatalytic Oxygen Reduction. ACS Applied Materials & Interfaces, 2018, 10, 8155-8164.	8.0	20
104	An Electrochemical Biosensor with Dual Signal Outputs: Toward Simultaneous Quantification of pH and O ₂ in the Brain upon Ischemia and in a Tumor during Cancer Starvation Therapy. Angewandte Chemie, 2017, 129, 10607-10611.	2.0	19
105	Amorphous Y(OH) ₃ -promoted Ru/Y(OH) ₃ nanohybrids with high durability for electrocatalytic hydrogen evolution in alkaline media. Chemical Communications, 2018, 54, 12202-12205.	4.1	19
106	Bovine serum albumin encapsulation of near infrared fluorescent nano-probe with low nonspecificity and cytotoxicity for imaging of HER2-positive breast cancer cells. Talanta, 2020, 210, 120625.	5.5	19
107	CuO/Ag ₂ S/CuS Nanohybridsâ€Integrated Photoelectric and Photothermal Effects for Ultrasensitive Detection of Inorganic Pyrophosphatase. Advanced Functional Materials, 2022, 32, 2106854.	14.9	19
108	Preparation of Reactive Oligo(<i>p</i> â€Phenylene Vinylene) Materials for Spatial Profiling of the Chemical Reactivity of Intracellular Compartments. Advanced Materials, 2016, 28, 3749-3754.	21.0	18

#	Article	IF	CITATIONS
109	Nanostructured metal chalcogenides confined in hollow structures for promoting energy storage. Nanoscale Advances, 2020, 2, 583-604.	4.6	18
110	Coâ€Quenching Effect between Lanthanum Metal–Organic Frameworks Luminophore and Crystal Violet for Enhanced Electrochemiluminescence Gene Detection. Small, 2021, 17, e2103424.	10.0	18
111	Oxygen-Vacancy-Rich NiMnZn-Layered Double Hydroxide Nanosheets Married with Mo ₂ CT _{<i>x</i>} MXene for High-Efficiency All-Solid-State Hybrid Supercapacitors. ACS Applied Energy Materials, 2022, 5, 3346-3358.	5.1	17
112	Colloidal-sized zirconium porphyrin metal–organic frameworks with improved peroxidase-mimicking catalytic activity, stability and dispersity. Analyst, The, 2020, 145, 3002-3008.	3.5	16
113	Detection of NADH and Ethanol at Titanium Containing MCM-41 with Low Overpotential. Electroanalysis, 2007, 19, 1591-1596.	2.9	15
114	Versatile Synthesis of Pdâ^'M (M=Cr, Mo, W) Alloy Nanosheets Flowerâ€like Superstructures for Efficient Oxygen Reduction Electrocatalysis. ChemCatChem, 2020, 12, 4138-4148.	3.7	14
115	Highly sensitive and selective colorimetric sensor for thiocyanate based on electrochemical oxidation-assisted complexation reaction with Gold nanostars etching. Journal of Hazardous Materials, 2020, 391, 122217.	12.4	14
116	A versatile switchable dual-modal colorimetric and photoelectrochemical biosensing strategy <i>via</i> light-controlled sway of a signal-output transverter. Chemical Communications, 2021, 57, 3223-3226.	4.1	14
117	Monoclinic Copper(I) Selenide Nanocrystals and Copper(I) Selenide/Palladium Heterostructures: Synthesis, Characterization, and Surface-Enhanced Raman Scattering Performance. European Journal of Inorganic Chemistry, 2015, 2015, 2229-2236.	2.0	13
118	Facile Synthesis of <scp>Mo₂C</scp> Nanocrystals Embedded in Nanoporous Carbon Network for Efficient Hydrogen Evolution. Chinese Journal of Chemistry, 2017, 35, 911-917.	4.9	12
119	Substrate specificity-enabled terminal protection for direct quantification of circulating MicroRNA in patient serums. Chemical Science, 2019, 10, 5616-5623.	7.4	12
120	Nickel-mediated allosteric manipulation of G-quadruplex DNAzyme for highly selective detection of histidine. Analytica Chimica Acta, 2018, 1008, 90-95.	5.4	11
121	Spectrum-Quantified Morphological Evolution of Enzyme-Protected Silver Nanotriangles by DNA-Guided Postshaping. Journal of the American Chemical Society, 2019, 141, 19533-19537.	13.7	11
122	Mesoporous SiO2–(l)-lysine hybrid nanodisks: direct electron transfer of superoxide dismutase, sensitive detection of superoxide anions and its application in living cell monitoring. RSC Advances, 2013, 3, 20456.	3.6	10
123	Controllable Mn-doped ZnO nanorods for direct assembly of a photoelectrochemical aptasensor. Analyst, The, 2017, 142, 2177-2184.	3.5	10
124	Fabrication of non-destructive and enhanced electrochemiluminescence interface for reusable detection of cell-released dopamine. Sensors and Actuators B: Chemical, 2019, 285, 438-444.	7.8	10
125	Catalytic Hydrogenation of Nitrophenols by Cubic and Hexagonal Phase Unsupported Ni Nanocrystals. ChemistrySelect, 2019, 4, 42-48.	1.5	10
126	Quantitative principal component analysis of multiple metal ions with lanthanide coordination polymer networks. Sensors and Actuators B: Chemical, 2021, 346, 130469.	7.8	10

#	Article	IF	CITATIONS
127	An ultrasensitive photoelectrochemical bioanalysis strategy for tumor markers based on the significantly enhanced signal of a bismuth oxyiodine microsphere/graphitic carbon nitride composite. Analyst, The, 2018, 143, 1775-1779.	3.5	9
128	Disordered photonics coupled with embedded nano-Au plasmonics inducing efficient photocurrent enhancement. Talanta, 2018, 176, 428-436.	5.5	7
129	Ultrasensitive determination of intracellular hydrogen peroxide by equipping quantum dots with a sensing layer via self-passivation. Nano Research, 2022, 15, 4350-4356.	10.4	7
130	Endonuclease cleavage combined with horseradish peroxidase-assisted signal amplification for electrochemical monitoring of DNA. Electrochemistry Communications, 2012, 22, 133-136.	4.7	6
131	Small-sized Ag nanocrystals: high yield synthesis in a solid–liquid phase system, growth mechanism and their successful application in the Sonogashira reaction. RSC Advances, 2012, 2, 6061.	3.6	6
132	Correction to Two-Dimensional Tin Selenide Nanostructures for Flexible All-Solid-State Supercapacitors. ACS Nano, 2014, 8, 6509-6509.	14.6	6
133	Macaroniâ€Like Blueâ€Gray Nb ₂ O ₅ Nanotubes for Highâ€Reversible Lithiumâ€lon Storage. Advanced Energy and Sustainability Research, 2021, 2, 2100028.	5.8	6
134	Cold–antibody nanocomposite thin film fabricated by a liquid–liquid interface technique and its application for the sensitive immunoassay of alpha-fetoprotein. Analytical Methods, 2013, 5, 1909.	2.7	5
135	Sensitive determination of formamidopyrimidine DNA glucosylase based on phosphate group-modulated multi-enzyme catalysis and fluorescent copper nanoclusters. Analyst, The, 2020, 145, 5174-5179.	3.5	5
136	Gram‣cale Synthesis of Multipod Pd Nanocrystals by a Simple Solid–Liquid Phase Reaction and Their Remarkable Electrocatalytic Properties. European Journal of Inorganic Chemistry, 2012, 2012, 3740-3746.	2.0	4
137	A label-free fluorescent adenosine triphosphate biosensor via overhanging aptamer-triggered enzyme protection and target recycling amplification. Analyst, The, 2016, 141, 4006-4009.	3.5	4
138	A novel electrochemiluminescence biosensor based on S-doped yttrium oxide ultrathin nanosheets for the detection of anti-Dig antibodies. Analyst, The, 2018, 143, 2997-3000.	3.5	4
139	Simulated enzyme inhibition-based strategy for ultrasensitive colorimetric biothiol detection based on nanoperoxidases. Chemical Communications, 2019, 55, 11543-11546.	4.1	4
140	A facile and sensitive colorimetric detection for RNase A activity based on target regulated protection effect on plasmonic gold nanoparticles aggregation. Science China Chemistry, 2020, 63, 860-864.	8.2	4
141	A nanoscaled Au–horseradish peroxidase composite fabricated by an interface reaction and its characterization, immobilization and biosensing. Analytical Methods, 2015, 7, 3466-3471.	2.7	1
142	An enzyme cascade sensor with resistance to the inherent intermediate product by logic-controlled peroxidase mimic catalysis. Chemical Communications, 2021, 57, 2089-2092.	4.1	1
143	Supercapacitors: 3D Porous Nanoarchitectures Derived from SnS/Sâ€Doped Graphene Hybrid Nanosheets for Flexible Allâ€&olidâ€&tate Supercapacitors (Small 12/2017). Small, 2017, 13, .	10.0	0